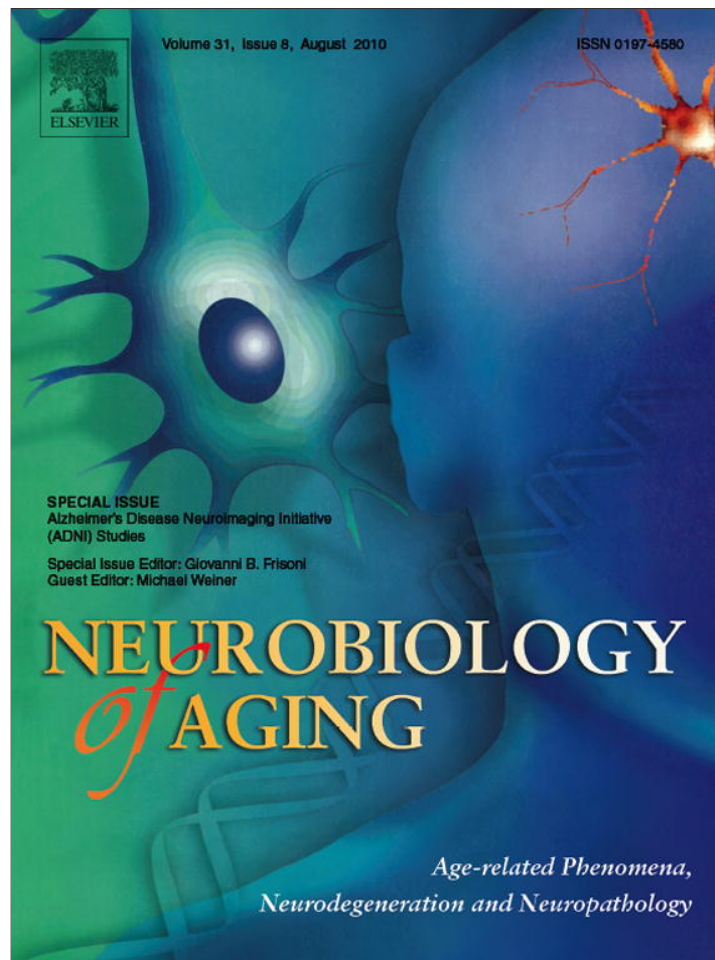


Provided for non-commercial research and education use.  
Not for reproduction, distribution or commercial use.



This article appeared in a journal published by Elsevier. The attached copy is furnished to the author for internal non-commercial research and education use, including for instruction at the authors institution and sharing with colleagues.

Other uses, including reproduction and distribution, or selling or licensing copies, or posting to personal, institutional or third party websites are prohibited.

In most cases authors are permitted to post their version of the article (e.g. in Word or Tex form) to their personal website or institutional repository. Authors requiring further information regarding Elsevier's archiving and manuscript policies are encouraged to visit:

<http://www.elsevier.com/copyright>



ELSEVIER

Neurobiology of Aging 31 (2010) 1340–1354

---



---

**NEUROBIOLOGY  
OF  
AGING**


---



---

www.elsevier.com/locate/neuaging

## Relations between brain tissue loss, CSF biomarkers, and the ApoE genetic profile: a longitudinal MRI study

Duygu Tosun<sup>a,\*</sup>, Norbert Schuff<sup>a,b</sup>, Diana Truran-Sacrey<sup>a</sup>, Leslie M. Shaw<sup>c</sup>, John Q. Trojanowski<sup>c</sup>, Paul Aisen<sup>d</sup>, Ronald Peterson<sup>e</sup>, Michael W. Weiner<sup>a,b</sup>, and the Alzheimer's Disease Neuroimaging Initiative

<sup>a</sup> Center for Imaging of Neurodegenerative Diseases, Department of Veterans Affairs Medical Center, San Francisco, CA, United States

<sup>b</sup> Department of Radiology, University of California, San Francisco, CA, United States

<sup>c</sup> Department of Pathology and Laboratory Medicine, Medicine at the Hospital of the University of Pennsylvania, Philadelphia, PA, United States

<sup>d</sup> Department of Neuroscience, University of California, San Diego, La Jolla, CA, United States

<sup>e</sup> Department of Neurology, Mayo Clinic College of Medicine, Rochester, MN, United States

Received 16 February 2010; received in revised form 26 April 2010; accepted 27 April 2010

### Abstract

Previously it was reported that Alzheimer's disease (AD) patients have reduced beta amyloid ( $A\beta_{1-42}$ ) and elevated total tau (t-tau) and phosphorylated tau (p-tau<sub>181p</sub>) in the cerebrospinal fluid (CSF), suggesting that these same measures could be used to detect early AD pathology in healthy elderly individuals and those with mild cognitive impairment (MCI). In this study, we tested the hypothesis that there would be an association among rates of regional brain atrophy, the CSF biomarkers  $A\beta_{1-42}$ , t-tau, and p-tau<sub>181p</sub> and apolipoprotein E (ApoE)  $\epsilon 4$  status, and that the pattern of this association would be diagnosis-specific. Our findings primarily showed that lower CSF  $A\beta_{1-42}$  and higher tau concentrations were associated with increased rates of regional brain tissue loss and the patterns varied across the clinical groups. Taken together, these findings demonstrate that CSF biomarker concentrations are associated with the characteristic patterns of structural brain changes in healthy elderly and mild cognitive impairment subjects that resemble to a large extent the pathology seen in AD. Therefore, the finding of faster progression of brain atrophy in the presence of lower  $A\beta_{1-42}$  levels and higher tau levels supports the hypothesis that CSF  $A\beta_{1-42}$  and tau are measures of early AD pathology. Moreover, the relationship among CSF biomarkers, ApoE  $\epsilon 4$  status, and brain atrophy rates are regionally varying, supporting the view that the genetic predisposition of the brain to beta amyloid and tau mediated pathology is regional and disease stage specific.

© 2010 Elsevier Inc. All rights reserved.

**Keywords:** MRI; Alzheimer's disease; Cerebrospinal fluid; Biomarkers; Cortical thickness; Atrophy; Brain tissue volume; ApoE; Mild cognitive impairment; Healthy aging

### 1. Introduction

There is an increasing body of evidence from in vivo imaging and postmortem studies indicating that Alzheimer's disease (AD) is associated with a sequence of pathophysiological events that can occur over a long period of

time (approximately 20 years) before clinical symptoms become apparent (Price and Morris, 1999). A slow disease progression potentially provides a window for early interventions to reduce or even stop progression of AD. Histopathological studies showed that the hallmarks of the disease, beta amyloid ( $A\beta$ )-rich amyloid plaques and neurofibrillary tangles formed by abnormal tau, precede neuron loss in presymptomatic AD patients (Price and Morris, 1999). Substantial accumulations of plaques and tangles in the brain can also be found in nondemented subjects with mild cognitive impairment (MCI), a transitional stage be-

\* Corresponding author at: Center for Imaging Neurodegenerative Diseases, Department of Veterans Affairs, Medical Center, 4150 Clement St., Bldg. 13, 114M, San Francisco, CA 94121, United States. Tel.: +1 415 221 4810 × 4800; fax: +1 415 668 2864.

E-mail address: duygu.tosun@ucsf.edu (D. Tosun).

tween normal aging and dementia (Aizenstein et al., 2008; Jack et al., 2009; Mintun et al., 2006). Consistent with histopathological findings, cerebrospinal fluid (CSF) chemistry studies have pointed to alterations in CSF  $A\beta$  (in particular  $A\beta_{1-42}$ ), total tau (t-tau), and phosphorylated tau (p-tau<sub>181p</sub>) concentrations preceding clinical symptoms of AD (Fjell et al., 2008). In general, studies found that increased CSF t-tau and p-tau<sub>181p</sub> were associated with neuronal and axonal damage, whereas reduced CSF  $A\beta_{1-42}$ , the form of  $A\beta$  that most readily fibrillizes and deposits earliest in plaques, has been implicated to reflect higher amyloid plaque burden in the brain (Clark et al., 2003; Shaw et al., 2009). However, the CSF measures are not easily interpretable because their origins are not exclusively brain derived and they provide no information about the regional spread of brain damage. Despite this, there is considerable agreement that measuring CSF  $A\beta_{1-42}$ , t-tau, and p-tau<sub>181p</sub> improves the diagnostic accuracy for AD (Andreasen et al., 1999).

Independent of biomarker studies, numerous structural magnetic resonance imaging (MRI) studies have shown a characteristic pattern of brain atrophy in AD and a similar pattern in MCI, primarily affecting regions in the parieto-temporal lobe, including the hippocampus, which plays a central role in memory formation (Chetelat and Baron, 2003; deToledo-Morrell et al., 2004; Du et al., 2001, 2002; Duarte et al., 2006; Hua et al., 2008; Kramer et al., 2004; Morra et al., 2008, 2009a, 2009b; Schroeter et al., 2009; Thompson et al., 2004; Whitwell et al., 2007, 2008). In addition, an increasing number of longitudinal MRI studies show that both AD and MCI are also associated with a regional pattern of increased rates of brain tissue loss compared with normal aging (Desikan et al., 2008; Du et al., 2003, 2004; Jack et al., 2004, 2005, 2008b; Stoub et al., 2005). With the emerging findings of CSF biomarker and structural imaging alterations in AD, there is considerable interest in utilizing the CSF and MRI measures together to improve detection of early signs of AD, as well as, in unraveling relationships between CSF  $A\beta_{1-42}$ , t-tau, and p-tau<sub>181p</sub> and MRI measures of regional brain alterations. Recently it has been shown that the combination of CSF biomarkers and atrophy rates can provide better prediction of AD than either source of data alone (Brys et al., 2009; Vemuri et al., 2009a, 2009b). However, whether relationships between brain atrophy rates and CSF biomarkers help further to improve predictions has not fully been explored.

Moreover, the role of the apolipoprotein E allele  $\epsilon 4$  (ApoE  $\epsilon 4$ ) gene, a major risk factor for AD, ought to be considered for a comprehensive evaluation. Presence of ApoE  $\epsilon 4$  is related to abnormal CSF biomarker concentrations (Glodzik-Sobanska et al., 2009; Sunderland et al., 2004), as well as to higher rates of brain atrophy (Basso et al., 2006; Fleisher et al., 2005; Potkin et al., 2009; Schuff et al., 2009; Sluimer et al., 2008). The relationships among all 3 factors, CSF biomarkers, ApoE  $\epsilon 4$ , and rates of regional

brain atrophy, might therefore provide important information about the vulnerability of the brain to AD. Our overall goal in this study was therefore to unravel the relationships among all 3 factors: brain atrophy rates, CSF biomarker concentrations, and presence of ApoE  $\epsilon 4$ . Toward the goal of identifying an AD biomarker, it will be important to fully understand the relationship between CSF biomarker concentrations and brain degeneration, such as neuron loss, which is thought to underlie the clinical symptoms in AD (Fjell et al., 2008; Jack et al., 2009). While CSF biomarkers relate to cumulative AD pathology in the brain as peripheral measures, MRI as an external tool to elucidate the distribution of the AD related neurodegeneration (i.e., brain atrophy in terms of tissue loss and ventricular enlargement). However, relatively few MRI studies so far have reported correlations between CSF biomarkers and the pattern of brain atrophy or the rate of atrophy progression (Fagan et al., 2009; Fjell et al., 2010a, 2010b; Hampel et al., 2005; Henneman et al., 2009; Herukka et al., 2008; Leow et al., 2009; Schuff et al., 2009). Specifically, in healthy elderly individuals, it has been shown that low CSF levels of  $A\beta_{1-42}$  correlate with ventricular expansion and volumetric reductions in widespread brain areas (Fjell et al., 2010a). In individuals with progressive MCI, low CSF  $A\beta_{1-42}$  concentration and high concentrations of CSF p-tau<sub>181p</sub> and t-tau are associated with higher subsequent rates of hippocampal atrophy (Hampel et al., 2005; Henneman et al., 2009; Herukka et al., 2008; Schuff et al., 2009). In AD patients, elevated CSF p-tau<sub>181p</sub> concentrations were associated with higher subsequent rates of hippocampal atrophy and medial temporal atrophy (Hampel et al., 2005; Henneman et al., 2009; Herukka et al., 2008; Leow et al., 2009), while low CSF  $A\beta_{1-42}$  concentrations exhibited larger rates of medial temporal atrophy (Leow et al., 2009). However, the majority of previous MRI studies in this context focused on hippocampal and temporal lobe atrophy and ventricular expansion in MCI and AD patients, while relatively little is known about relations between the CSF biomarker concentrations and atrophy rates of other regions throughout the brain. In addition, variations in these relationships across the spectrum of cognitive impairments have not been comprehensively studied for regions across the brain.

Our main goal in this study was to test the hypothesis that relations between CSF biomarkers (i.e.,  $A\beta_{1-42}$ , t-tau, and p-tau<sub>181p</sub> concentrations) and rates of regional brain atrophy not only vary across brain regions but also across the cognitive spectrum, including healthy elderly individuals (CN), individuals with MCI, and AD patients. In particular we tested that: (1) low  $A\beta_{1-42}$  and high t-tau and p-tau<sub>181p</sub> concentrations were associated with smaller mean regional brain tissue volume and cortical thickness in CN, MCI, and AD; (2) low  $A\beta_{1-42}$  and high t-tau and p-tau<sub>181p</sub> concentrations were associated with increased rates of regional brain atrophy in CN, MCI, and AD; and (3) the patterns of association were group-specific. In addition, we tested

whether abnormal CSF biomarker concentrations and ApoE  $\epsilon 4$  status separately or together were associated with higher rates of brain atrophy.

## 2. Methods

We examined the baseline regional tissue volume and cortical thickness, and the rate of change in regional tissue volume and cortical thickness across the brain in CN, individuals with MCI, and AD patients. Structural magnetic resonance imaging (MRI) brain scans at multiple time points (4 time point scans — baseline, 6, 12, and 24 months — for CN and AD patients and 5 time point scans — baseline, 6, 12, 18, and 24 months — for individuals with MCI) were acquired at multiple Alzheimer's Disease Neuroimaging Initiative (ADNI) sites using 1.5 Tesla MRI scanners. Using FreeSurfer ([surfer.nmr.mgh.harvard.edu/fswiki](http://surfer.nmr.mgh.harvard.edu/fswiki)) longitudinal processing framework, regional tissue volumes of a total of 108 cortical and subcortical regions and local cortical thickness throughout the entire cortex were automatically measured at each time point. In each diagnostic group separately, generalized linear mixed effect models followed by pair-wise maximum likelihood test were performed to test: (1) if baseline CSF biomarker concentrations predict absolute volumes and local thickness at baseline; (2) if baseline CSF biomarker concentrations modulate the rates of brain atrophy; and (3) if CSF biomarkers and ApoE  $\epsilon 4$  modulate the rates of brain atrophy jointly or independently, after accounting for variations in age, sex, and education. Pursuing a region-of-interest based analysis allows us to study the subcortical structures while surface-based cortical thickness analysis provides better localization of the effects on cortical mantle. Finally, we tested if the observed modulation effects of baseline CSF biomarkers on rates of atrophy differ among groups. The methodological details are explained herein.

### 2.1. Participants

The participants in this study were recruited through the ADNI, a longitudinal, multicenter study launched in 2003 by the National Institute on Aging (NIA), the National Institute of Biomedical Imaging and Bioengineering (NIBIB), the Food and Drug Administration (FDA), private pharmaceutical companies, and nonprofit organizations, as a \$60 million, 5-year, public-private partnership to define biomarkers of early Alzheimer's disease for clinical trials ([www.adni-info.org](http://www.adni-info.org)). The Principal Investigator of this initiative is Michael W. Weiner, MD of the Veteran Affairs Medical Center and University of California in San Francisco.

Briefly, inclusion criteria for the CN group were Mini Mental State Examination (MMSE) scores between 24 and 30, a Clinical Dementia Rating-Sum of Boxes (CDR-SB) score of 0, and lack of depression, MCI, or dementia. Inclusion criteria for the MCI group followed the Peterson

Table 1  
Demographic features of study groups

	CN	MCI	AD
<i>n</i> (baseline)	77	119	54
<i>n</i> follow-up (6, 12, 18, and 24 months)	77, 76, 0, 63	119, 109, 96, 77	54, 53, 0, 31
Baseline age (years)	75 ± 5.0	74 ± 7.6	74 ± 8.0
Gender (F/M)	40/37	46/73	25/29
Baseline CSF A $\beta$ <sub>1–42</sub> (pg/mL)	203 ± 51.8	165 ± 57.5	142 ± 39.7
Baseline CSF t-tau (pg/mL)	70 ± 29.5	101 ± 50.0	128 ± 53.1
Baseline CSF p-tau <sub>181p</sub> (pg/mL)	26 ± 15.0	35 ± 16.5	42 ± 16.8
ApoE $\epsilon 4$ status (carrier %)	29%	54%	67%

Data are given as mean ± standard deviation.

Key: A $\beta$ , beta amyloid; AD, Alzheimer's disease; ApoE, apolipoprotein E; CN, healthy elderly; CSF, cerebrospinal fluid; F, female; M, male; MCI, mild cognitive impairment; p-tau, phosphorylated tau; t-tau, total tau.

criteria (Petersen et al., 1999) for amnesic MCI, which required a subjective memory complaint, objective memory loss measured by education-adjusted Wechsler Memory Scale-Revised Logical Memory II scores, a CDR-SB of 0.5, absence of significant impairment in other cognitive domains, preserved activities of daily living, and an absence of dementia. AD participants met the National Institute for Neurological and Communicative Disorders and Stroke-Alzheimer's Disease and Related Disorder Association (NINDS/ADRDA) criteria for probable AD, had a Mini Mental State Examination score between 18 and 26, and a CDR-SB of 0.5 to 1.0. Exclusion criteria included history of structural brain lesions or head trauma, significant neurological disease other than incipient AD, and use of psychotropic medications that could affect memory. The full details of the inclusion and exclusion criteria for the ADNI can be found at [www.adni-info.org](http://www.adni-info.org). Written consent was obtained from all subjects participating in the study according to the Declaration of Helsinki, and the study was approved by the institutional review board at each participating site.

The population in this study included ADNI subjects with valid test results for all 3 CSF biomarkers and successful longitudinal FreeSurfer processing of magnetic resonance (MR) images from at least 2 time points. Overall, the study population was comprised of 77 CN, 118 MCI, and 53 AD subjects. Details of CSF biomarker concentration measurement and longitudinal structural MR image processing are described in the following sections. The demographic details of each group are given in Table 1.

### 2.2. Structural MRI acquisition

The participants underwent a standardized 1.5 Tesla MRI protocol ([www.loni.ucla.edu/ADNI/Research/Cores/index.shtml](http://www.loni.ucla.edu/ADNI/Research/Cores/index.shtml)), which included 2 T1-weighted MRI scans using a sagittal volumetric magnetization prepared rapid gradient

echo (MP-RAGE) sequence with the following acquisition parameters: echo time (TE) of 4 ms, repetition time (TR) of 9 ms, flip angle of 8°, acquisition matrix size of  $256 \times 256 \times 166$  in the x-, y- and z-dimensions with a nominal voxel size of  $0.94 \times 0.94 \times 1.2 \text{ mm}^3$ . Only 1 of the MP-RAGE sets was used for the analysis. The ADNI MRI quality control center at the Mayo Clinic selected the MP-RAGE image with higher quality and corrected for system-specific image artifacts, as described in Jack et al. (2008a).

### 2.3. CSF biomarker concentrations

CSF samples were obtained from 53% of ADNI participants, while the rest did not undergo lumbar puncture. The demographics of ADNI subjects with CSF samples are comparable with that in the full ADNI patient population ([www.adni-info.org](http://www.adni-info.org)).

A small sample of CSF from the lower spine of each subject was collected at baseline by lumbar puncture in the morning after an overnight fast. Lumbar puncture was performed with a 20- or 24-gauge spinal needle as described in the ADNI procedures manual ([www.adni-info.org](http://www.adni-info.org)). In brief, CSF was collected into collection tubes provided to each site, then transferred into polypropylene transfer tubes followed by freezing on dry ice within 1 hour after collection, and shipped overnight to the ADNI Biomarker Core laboratory at the University of Pennsylvania Medical Center on dry ice. Aliquots of 0.5 mL were prepared from these samples after thawing for 1 hour at room temperature and gentle mixing. The aliquots were stored in bar code-labeled polypropylene vials at  $-80 \text{ }^\circ\text{C}$ .  $A\beta_{1-42}$ , t-tau, and p-tau<sub>181p</sub> were measured in each aliquot using the multiplex xMAP Luminex platform (Luminex, Corp, Austin, Texas) with Innogenetics (INNO-BIA AlzBio3; Ghent, Belgium; for research use only reagents) immunoassay kit-based reagents. Full details of this combination of immunoassay reagents and analytical platform are provided elsewhere (Olsson et al., 2005). The ADNI baseline CSF samples were analyzed over a 14-day period and included test-retest analyses of 29 of the samples that further substantiated the analytical performance ( $r^2$  values for comparison of the initial test result with retest result were 0.98, 0.90, and 0.85 for t-tau,  $A\beta_{1-42}$ , and p-tau<sub>181p</sub>, respectively for 29 randomly selected samples). Full details of ADNI baseline CSF biomarker measurements are provided elsewhere (Shaw et al., 2009).

### 2.4. FreeSurfer longitudinal MR image processing

Automated cortical thickness measures, cortical parcellation, and subcortical segmentation were performed with FreeSurfer software package, version 4.4 ([surfer.nmr.mgh.harvard.edu/fswiki](http://surfer.nmr.mgh.harvard.edu/fswiki)). To reduce the confounding effect of intrasubject morphological variability, each subject's longitudinal data series was processed by FreeSurfer longitudinal workflow. The longitudinal workflow was designed to estimate brain morphometry measurements that were unbiased

with respect to any time point. Instead of using information from a specific time point as a prior for other time points, a template image volume was created as an unbiased prior for all time points.

FreeSurfer longitudinal workflow consists of 4 stages: (1) processing of all time points individually with the cross-sectional workflow; (2) creation of a probabilistic template unbiased toward time points from all time points' cross-sectional data; (3) processing of unbiased template with the cross-sectional workflow; and finally, (4) reprocessing of each time point with the longitudinal workflow, which uses the unbiased template results as initial guess for the segmentation and surface reconstruction. For a full description of the FreeSurfer processing steps, see Fischl et al. (2002, 2004), and for a full description of the longitudinal workflow, see [surfer.nmr.mgh.harvard.edu/fswiki/LongitudinalProcessing](http://surfer.nmr.mgh.harvard.edu/fswiki/LongitudinalProcessing).

The FreeSurfer measures for each subject at each time point are as follows: (1) each image voxel in MR image volume was automatically assigned one of 40 neuroanatomical labels and for each anatomical subcortical region of interest (ROI) total tissue volume was estimated (Fischl et al., 2002). (2) Vertex-based cortical thickness measurements were obtained as the distance between the reconstructed surface representations of the gray matter/white matter and white matter/CSF tissue interfaces (Fischl and Dale, 2000). Each cortical surface was spatially normalized to a template cortical surface using a nonrigid high-dimensional spherical averaging method to align cortical folding patterns. Subject cortical thickness maps were mapped onto the template surface based on this spatial normalization and then smoothed by a surface-based Gaussian blurring kernel with a standard deviation of 10 mm to remove noise-induced variations in the measurements. (3) Spatial normalization to the template cortical surface was also used to automatically parcellate the subject cortical surfaces at each time point to 34 anatomical regions per cortical hemisphere (Fischl et al., 2004). For each cortical ROI, cortical gray matter volume was estimated based on the cortical parcellation and tissue segmentation.

The surface reconstruction, subcortical segmentation, and cortical parcellation results were visually examined for anatomical accuracy. Although the FreeSurfer software package allows for manual editing to correct registration and segmentation errors, given the large number of subjects in the ADNI dataset, only the data with accurate results from fully automated processing were used in the subsequent analysis in the interest of a practical total processing time and avoidance of reader bias. Seventy-four percent of the MR images passed this quality control, 3% of the images failed the quality control completely, and remaining 23% of the images received a partial pass on the quality control. Details of the quality control procedure are posted online at [www.loni.ucla.edu/twiki/pub/ADNI/ADNIPostProc/UCSFFreeSurferMethodsSummary.pdf](http://www.loni.ucla.edu/twiki/pub/ADNI/ADNIPostProc/UCSFFreeSurferMethodsSummary.pdf).

## 2.5. Statistical analyses

For each subject, variations in brain volumes or cortical thickness were modeled as a function of time starting with the baseline scan (time point 0) in intervals of subsequent MRI scans in units of years. We employed a general linear mixed effects (GLME) model for the analysis of the longitudinal data in which the response variable (i.e., cortical thickness or tissue volumes of cortical and subcortical regions) was regressed against the explanatory variables including time, baseline CSF biomarker concentration (i.e.,  $A\beta_{1-42}$ , p-tau<sub>181p</sub>, or t-tau), and the interaction between time and baseline CSF biomarker concentration to estimate the fixed effects in the group, separately from the random effects such as within subject variations in both baseline and longitudinal measures. This concept was used to test the primary hypothesis that variations in CSF biomarker concentrations modulate rates of brain atrophy (i.e., cortical thinning, tissue volume loss, or ventricular expansion). The fixed effect model was formulated as follows:

$$V_{ij} = \beta_0 + \beta_{Years}T_{ij} + \beta_{CSFbio}B_{i0} + \beta_{Years:CSFbio}T_{ij}B_{i0} + \varepsilon_{ij}$$

Here,  $V_{ij}$  represents the size of a brain structure (volume or thickness) from subject  $i$  at time point  $j$ . Accordingly,  $T_{ij}$  indicates the time point of the individual MRI scan,  $B_{i0}$  represents individual CSF biomarker concentrations at baseline and  $\varepsilon_{ij}$  is the mixed effects error. Our goal was to test the significance of the coefficient  $\beta_{Years:CSFbio}$  in explaining structural variations (i.e., the moderator) relative to the coefficients  $\beta_0$ ,  $\beta_{Years}$ , and  $\beta_{CSFbio}$  and independent of random variations in brain structures at baseline and over time. For a significant interaction to occur, CSF biomarker concentration must modulate the relationship between time and the response variable (i.e., local cortical thickness or regional tissue volume). To determine if the addition of an interaction term ( $\beta_{Years:CSFbio}$ ) between rates of brain atrophy and CSF biomarkers in the model significantly improves the explanatory power of regional variations in cortical thickness or brain tissue volume as a function of biomarkers, we compared pair-wise GLME models (i.e., with and without the  $\beta_{Years:CSFbio}$  term), fitted by maximum likelihood (ML) via  $F$ -tests. These tests were performed separately for each group (i.e., CN, MCI, and AD). Similarly, to determine the significance of CSF biomarker effects on regional tissue volumes and cortical thickness at baseline, the additive term  $\beta_{CSFbio}$  was assessed by pair-wise comparisons of GLME models with and without  $\beta_{CSFbio}$  term, followed by maximum likelihood (ML) via  $F$ -tests. Each CSF biomarker was centered on its population mean to reduce colinearity.

To assess if the effect of CSF biomarkers on rates of regional brain atrophy differ across groups (CN, MCI, and AD), we resampled the random effects residual of the fits by 100-fold bootstrap and evaluated differences in distributions by analysis of variance.

Finally, we tested the extent to which ApoE  $\varepsilon 4$  status contributes to higher brain atrophy rates independent of the CSF biomarker concentrations (ApoE  $\varepsilon 4$  status + CSF biomarker) or via a synergistic interaction with the biomarkers (ApoE  $\varepsilon 4$  status  $\times$  CSF biomarker). Again, pair-wise ML tests were performed between models with and without the interaction term (i.e., ApoE  $\varepsilon 4 \times$  CSF biomarker) to determine the contribution of the interaction.

Age, gender, and education were included as covariates in each regression model described above. For cortical thickness measures, the GLME models and the corresponding pair-wise ML  $F$ -tests were evaluated at each surface vertex independently. All statistical analyses were computed using R (the R Project for Statistical Computing; [www.r-project.org](http://www.r-project.org)). To control for false positive findings given the large number of comparisons per brain map, we used the concept of a false discovery rate (FDR) at the level  $q = 0.05$  (Benjamini and Hochberg, 1995). For testing the a priori hypotheses, which comprised a limited number of planned tests, we used a per comparison error rate of  $q = 0.05$  for each test to determine the probability that any one contrast, after passing FDR, is found by chance.

## 3. Results

### 3.1. Effects of baseline CSF biomarker concentrations on regional mean tissue volumes

The results of associations between biomarkers and mean regional brain tissue volumes (i.e.,  $\beta_{CSFbio}$  coefficient) are summarized in Table 2 for those cortical and subcortical ROIs where the baseline CSF biomarker concentrations had significant effect on mean regional tissue volumes (FDR corrected  $p < 0.05$ ). Listed are both the coefficients from the GLME models (representing change in tissue volume per unit biomarker concentration, i.e.,  $\text{mm}^3/(\text{pg/mL})$ ) and the likelihood ratio (LR) of the biomarker effects. Variations in baseline CSF biomarker concentrations in the CN group were not significantly associated with mean regional brain volumes. In contrast, higher baseline concentrations of CSF t-tau and p-tau<sub>181p</sub> in MCI were associated with smaller caudate volumes. In AD, lower baseline concentrations of CSF  $A\beta_{1-42}$  were associated with smaller baseline gray matter volumes in lingual, pericalcarine, and postcentral cortices.

### 3.2. Effects of baseline CSF biomarkers concentrations on the rates of regional tissue volume change

Lower concentrations of CSF  $A\beta_{1-42}$  were associated: (1) in CN with increased rates of ventricular enlargement; (2) in MCI with increased rates of ventricular enlargement and increased rates of atrophy prominently in the left lateral and medial temporal cortices, left hippocampus, left isthmus cingulate, and right amygdala; and (3) in AD with decreased rates of atrophy in the caudate and accumbens area. The interaction coefficient of the GLME models (representing change in the rates of atrophy per unit biomarker concen-

Table 2

Effects of baseline CSF biomarkers on the mean regional tissue volumes (in units of mm<sup>3</sup>/[pg/mL])

Region	$\beta_{A\beta_{1-42}}$	LR	$\beta_{t\text{-tau}}$	LR	$\beta_{p\text{-tau}_{181p}}$	LR
Individuals with mild cognitive impairment (MCI)						
Right caudate	—	—	$-4.0 \pm 0.9^a$	19.6	$-10.1 \pm 2.9^b$	13.4
Left caudate	—	—	$-3.8 \pm 0.9^a$	19.5	—	—
Patients with Alzheimer's disease (AD)						
Left lingual	$11.0 \pm 2.3^a$	20.8	—	—	—	—
Right pericalcarine	$3.8 \pm 1.0^b$	11.7	—	—	—	—
Right cerebral cortex	$144.8 \pm 42.8^b$	10.9	—	—	—	—
Right lingual	$7.0 \pm 2.3^b$	10.3	—	—	—	—
Left postcentral	$11.4 \pm 3.5^b$	9.4	—	—	—	—

Data are given as mean  $\pm$  standard deviation. Nonsignificant effects are indicated by —.

Key: CSF, cerebrospinal fluid; LR, likelihood ratio.

<sup>a</sup>  $p < 0.05$ .

<sup>b</sup>  $p < 0.005$ .

tration, i.e., mm<sup>3</sup>/(year  $\times$  pg/mL)) as well as the likelihood ratio of  $A\beta_{1-42}$  atrophy modulation effects are summarized in Table 3 for cortical and subcortical ROIs with significant effects only (FDR corrected  $p < 0.05$ ).

In contrast to baseline CSF  $A\beta_{1-42}$  concentrations, baseline concentrations of CSF t-tau were not significantly associated with any rate of brain volume changes in CN and MCI groups. In AD, however, higher concentrations of base-

Table 3

Effects of baseline CSF biomarkers on rates of regional brain volume loss (in units of mm<sup>3</sup>/[year  $\times$  pg/mL])

Region	$\beta_{\text{Years: } A\beta_{1-42}}$	LR	$\beta_{\text{Years: } t\text{-tau}}$	LR	$\beta_{\text{Years: } p\text{-tau}_{181p}}$	LR
Healthy elderly (CN)						
Right lateral ventricle	$-4.7 \pm 0.8^a$	31.1	—	—	$12.2 \pm 3.0^b$	16.1
Left lateral ventricle	$-4.3 \pm 0.8^a$	27.0	—	—	—	—
Right inferior lateral ventricle	—	—	—	—	$1.6 \pm 0.4^b$	16.8
Individuals with mild cognitive impairment (MCI)						
Right lateral ventricle	$-5.6 \pm 1.2^a$	21.9	—	—	—	—
Left temporal pole	$0.4 \pm 0.1^b$	17.4	—	—	$-1.1 \pm 0.3^b$	13.1
Left lateral ventricle	$-5.6 \pm 1.4^b$	16.3	—	—	—	—
Left fusiform	$0.9 \pm 0.2^b$	16.3	—	—	—	—
Left inferior temporal	$1.1 \pm 0.3^b$	15.9	—	—	$-3.7 \pm 1.0^b$	14.1
Left entorhinal	$0.3 \pm 0.1^b$	15.9	—	—	$-1.0 \pm 0.2^b$	16.7
Left isthmus cingulate	$0.2 \pm 0.1^c$	12.5	—	—	—	—
Left hippocampus	$0.3 \pm 0.1^c$	11.7	—	—	$-0.9 \pm 0.3^c$	10.8
Right middle temporal	$1.0 \pm 0.3^c$	10.1	—	—	$-4.3 \pm 1.1^b$	15.6
Left parahippocampal	$0.2 \pm 0.1^c$	10.0	—	—	$-0.9 \pm 0.2^b$	13.2
Left inferior lateral ventricle	$-0.5 \pm 0.2^c$	9.4	—	—	—	—
Right inferior lateral ventricle	$-0.5 \pm 0.2^c$	9.2	—	—	—	—
Left cerebral cortex	$9.3 \pm 3.1^c$	9.1	—	—	—	—
Left middle temporal	$0.8 \pm 0.3^c$	9.1	—	—	$-2.7 \pm 0.9^c$	8.2
Right cerebral cortex	$8.8 \pm 2.9^c$	9.0	—	—	$-31.5 \pm 10.3^c$	0.4
Right fusiform	$0.8 \pm 0.2^c$	8.7	—	—	—	—
Third ventricle	$-0.2 \pm 0.1^c$	7.8	—	—	—	—
Right amygdala	$0.2 \pm 0.1^c$	7.0	—	—	—	—
Left amygdala	—	—	—	—	$-0.7 \pm 0.2^c$	12.7
Right inferior temporal	—	—	—	—	$-3.7 \pm 1.0^b$	13.6
Patients with Alzheimer's disease (AD)						
Left caudate	$-2.6 \pm 0.5^a$	24.2	$-1.3 \pm 0.4^c$	9.6	—	—
Right caudate	$-2.3 \pm 0.5^b$	18.7	$-1.3 \pm 0.4^c$	10.5	—	—
Right accumbens area	$-0.6 \pm 0.2^b$	14.7	—	—	—	—
Right isthmus cingulate	—	—	$0.6 \pm 0.1^b$	17.6	—	—
Right posterior cingulate	—	—	$0.7 \pm 0.2^c$	12.4	—	—
Right precuneus	—	—	$1.5 \pm 0.5^c$	11.1	—	—
Left lateral ventricle	—	—	$-8.0 \pm 2.4^c$	11.0	—	—

Data are given as mean  $\pm$  standard deviation. Nonsignificant effects are indicated by —.

Key: LR, likelihood ratio.

<sup>a</sup>  $p < 0.0005$ .

<sup>b</sup>  $p < 0.005$ .

<sup>c</sup>  $p < 0.05$ .

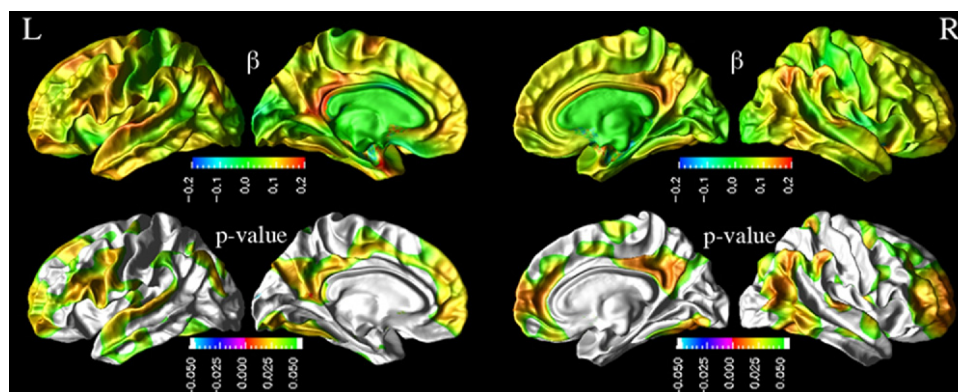


Fig. 1. Association between baseline cerebrospinal fluid (CSF) beta amyloid ( $A\beta$ )<sub>1-42</sub> concentrations and absolute cortical thickness in healthy elderly (CN) group. Top row: cortical maps of regression coefficients  $\beta_{A\beta 1-42}$  from general linear mixed effects (GLME) models. Bottom row: resulting false discovery rate (FDR) corrected  $p$ -value maps from pair-wise maximum likelihood (ML)  $F$  tests.

line CSF t-tau were associated with decreased rates of atrophy in the right posterior cingulate, isthmus cingulate, and precuneus cortices and ventricular enlargement, and increased rates of caudate atrophy as summarized in Table 3.

Finally, atrophy modulation effects of baseline CSF p-tau<sub>181p</sub> concentration largely mirrored the pattern seen for  $A\beta$ <sub>1-42</sub> in CN and MCI, though associations with baseline CSF p-tau<sub>181p</sub> involved fewer regions in MCI. Specifically, higher concentrations of CSF p-tau<sub>181p</sub> were associated: (1) with increased rates of ventricular enlargement in CN; (2) with increased rates of regional brain atrophy prominently in the left temporal lobe, hippocampus, and amygdala in MCI. In AD, however, baseline CSF p-tau<sub>181p</sub> concentrations were not associated with rate of any brain volume changes. Significant interaction coefficient of the GLME models as well as the likelihood ratio of p-tau modulation effects are summarized in Table 3.

### 3.3. Effects of baseline CSF biomarker concentrations on mean regional cortical thickness

Next, we report effects of CSF biomarker concentrations on mean cortical thickness after accounting for variations in age, gender, and education across subjects. Fig. 1 depicts the regional distribution of CSF  $A\beta$ <sub>1-42</sub> effects on mean cortical thickness for CN. Also shown in Fig. 1 is the regional distribution of the corresponding  $p$  values of the CSF  $A\beta$ <sub>1-42</sub> atrophy modulation effects based on the ML  $F$ -tests. In CN, lower baseline CSF  $A\beta$ <sub>1-42</sub> was associated with a thinner cortex in the left frontal pole, left rostral-middle frontal left superior frontal, left pars opercularis, left pars triangularis, left supramarginal, left inferior parietal, left superior temporal, left middle temporal, left inferior temporal, left posterior cingulate, left precuneus, left fusiform, right frontal pole, right rostral middle frontal, right supramarginal, right inferior parietal, right superior parietal, right middle temporal, right inferior temporal, right medial orbitofrontal, right posterior cingulate, right paracentral lobule, right precuneus, and right fusiform cortices. In MCI and

AD, no statistically significant association between the baseline CSF biomarker concentrations and the mean cortical thickness measures were observed.

Neither t-tau nor p-tau<sub>181p</sub> showed significant association with mean cortical thickness in CN, MCI, and AD groups.

### 3.4. Effects of baseline CSF biomarkers concentrations on the rates of regional cortical atrophy

Similarly, we report next the modulation effects of CSF biomarkers on the rates of cortical thinning after accounting for variations in age, gender, and education across subjects. Fig. 2 depicts the regional distribution of a CSF  $A\beta$ <sub>1-42</sub> modulation effect on the rates of cortical thinning for MCI. Also shown in Fig. 2 is the regional distribution of the corresponding  $p$  values of the CSF  $A\beta$ <sub>1-42</sub> atrophy modulation effects based on the ML  $F$ -tests. In MCI, lower concentrations of CSF  $A\beta$ <sub>1-42</sub> were associated with increased rates of cortical thinning throughout the cortex. The effects were statistically significant (FDR corrected;  $p < 0.05$ ) in the left temporal pole, left inferior temporal, left middle temporal, left inferior parietal, left paracentral lobule, left cingulate, left isthmus cingulate, left precuneus, left entorhinal, left fusiform, right inferior temporal, and right middle temporal cortices.

In Fig. 3 are shown the regional distribution of CSF p-tau<sub>181p</sub> effects on the rates of cortical thinning for MCI as well as the corresponding significance maps. The results indicate that higher baseline CSF p-tau<sub>181p</sub> concentrations in MCI were associated with higher rates of cortical thinning, significantly in the left temporal pole, left superior temporal sulcus, left entorhinal gyrus, right inferior, and middle temporal cortices. Similarly, higher baseline CSF t-tau concentrations were associated with higher cortical atrophy rates in the left entorhinal gyrus in MCI patients, as shown in Fig. 4.

Neither CN nor AD patients showed significant modulation effects of baseline CSF biomarkers on the cortical atrophy rates after correcting for multiple comparison. Although they are not statistically significant, cortical maps of

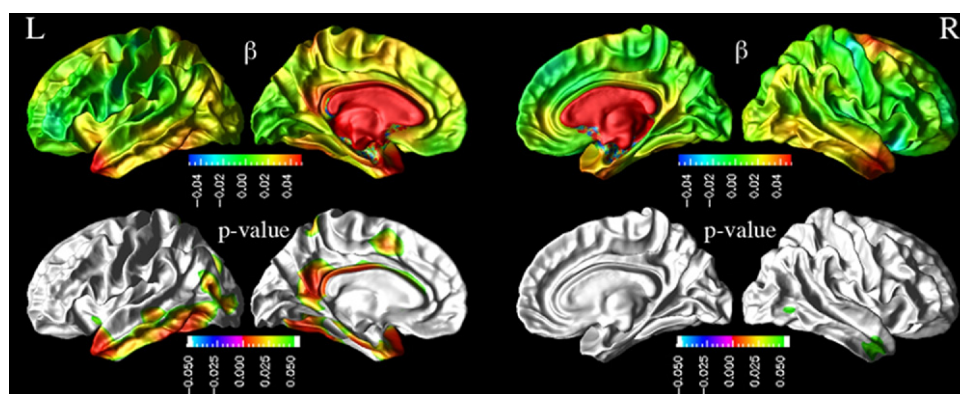


Fig. 2. Top row: distribution of effects of lower baseline cerebrospinal fluid (CSF) beta amyloid ( $A\beta_{1-42}$ ) concentrations on higher rate of cortical thinning in mild cognitive impairment (MCI) group, expressed in terms of a regression coefficient beta (in  $\text{mm}^3/[\text{year} \times \text{pg/uL}]$ ). Bottom row: also displayed are the corresponding significance maps ( $p$ -values, false discovery rate [FDR] corrected) derived from pair-wise maximum likelihood  $F$  tests between general linear mixed effects (GLME) models with and without an interaction between biomarker concentration and atrophy rate.

regression coefficients of  $\beta_{\text{Years:CSFbiomarker}}$  for CN and AD groups are provided in the Supplementary Figure.

### 3.5. Group differences in CSF biomarker effects on rates of cortical thinning

By bootstrapping the random effects residuals of the GLME fits with time and baseline CSF biomarker concentration interaction term, we tested if the estimates of the association between biomarkers and atrophy rates significantly differ across populations. Based on pair-wise group comparison, we found that differences in the estimations between the groups were all significant ( $p = 0.05$  level).

### 3.6. ApoE $\epsilon 4$ analyses

In our dataset, presence of ApoE  $\epsilon 4$  alleles correlated significantly with the CSF  $A\beta_{1-42}$  concentrations ( $r = -0.50, p < 10^{-5}$  in CN,  $r = -0.49, p < 10^{-8}$  in MCI, and  $r = -0.53, p < 10^{-5}$  in AD), after controlling for age. A partial correlation between presence of ApoE  $\epsilon 4$  alleles and  $p\text{-tau}_{181p}$  and  $t\text{-tau}$  after controlling for age was significant only in MCI group ( $r = 0.34$  with  $p < 10^{-3}$  and  $r = 0.39$  with  $p < 10^{-6}$ , respectively).

In the CN group, ML  $F$ -test showed that a higher rate of ventricular enlargement was associated independently with higher  $t\text{-tau}$  as well as presence of ApoE  $\epsilon 4$ , while lower CSF  $A\beta_{1-42}$  and higher  $p\text{-tau}_{181p}$  alone explained the increased rate of ventricular enlargement without a significant contribution from ApoE  $\epsilon 4$ .

In individuals with MCI, CSF biomarker concentrations (i.e., lower  $A\beta_{1-42}$ , higher  $p\text{-tau}_{181p}$ , and  $t\text{-tau}$ ) and ApoE  $\epsilon 4$  were independently associated with higher rates of ventricular enlargement and tissue volume loss in bilateral hippocampus, right amygdala, bilateral temporal lobe (i.e., middle temporal, inferior temporal, temporal pole, and fusiform), right lingual, left entorhinal, left parahippocampal, left isthmus cingulate, and left precuneus cortices. Similarly, lower CSF  $A\beta_{1-42}$  and ApoE  $\epsilon 4$  together were associated with higher rates of cortical thinning in temporoparietal cortex, including precuneus and posterior cingulate (Supplementary Figure II). CSF tau and ApoE  $\epsilon 4$  together were associated with higher rates of cortical thinning in the entorhinal cortex, precuneus and temporal pole (Supplementary Figure II). In contrast, lower  $A\beta_{1-42}$  alone

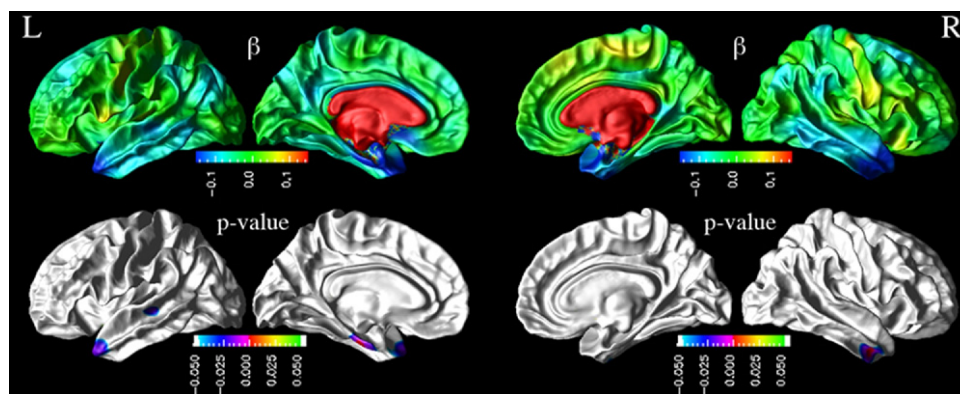


Fig. 3. Effects of baseline cerebrospinal fluid (CSF) phosphorylated tau ( $p\text{-tau}_{181p}$ ) concentrations on the rates of cortical atrophy in mild cognitive impairment (MCI) group. Top row: cortical maps of regression coefficients  $\beta_{\text{Years:p-tau181p}}$  from general linear mixed effects (GLME) models. Bottom row: resulting false discovery rate (FDR) corrected  $p$  value map from pair-wise maximum likelihood (ML)  $F$  tests.

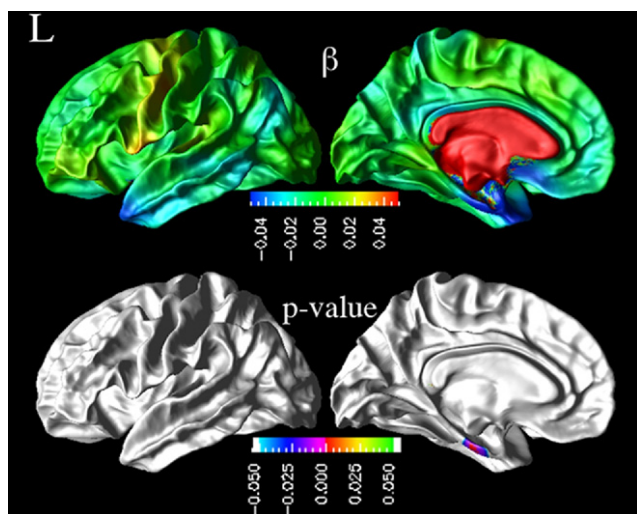


Fig. 4. Effects of baseline cerebrospinal fluid (CSF) total tau (t-tau) concentrations on rate of cortical atrophy in mild cognitive impairment (MCI) group. Top row: cortical maps of regression coefficients  $\beta_{\text{Years: t-tau}}$  from general linear mixed effects (GLME) models. Bottom row: resulting FDR corrected  $p$ -value map from pair-wise maximum likelihood (ML)  $F$  tests.

explained higher rates of tissue volume loss as well as cortical thinning in left entorhinal, fusiform, inferior temporal, temporal pole, and parahippocampal cortices without a significant contribution from ApoE  $\epsilon 4$ . Similarly, higher CSF tau explained higher rates of cortical thinning in entorhinal cortex without a significant contribution from ApoE  $\epsilon 4$ .

In patients with AD, lower  $A\beta_{1-42}$  and higher t-tau concentrations as well as presence of ApoE  $\epsilon 4$  were associated with higher rates of tissue volume loss in the left and right caudate. However, a higher rate of volume loss in the caudate was explained by lower  $A\beta_{1-42}$  alone without a significant contribution of ApoE  $\epsilon 4$  status. On the other, ApoE  $\epsilon 4$  alone was associated with a higher rate of volume loss in caudate, independent of the CSF t-tau concentration.

In no case did an interaction between ApoE  $\epsilon 4$  status and CSF biomarker concentration (i.e., ApoE  $\epsilon 4$  status  $\times$  CSF biomarker) approach significance in predicting rate of volume loss or cortical thinning.

#### 4. Discussion

We have 4 major findings: (1) in controls, an association between CSF  $A\beta_{1-42}$  and baseline cortical thickness was observed prominently in regions that generally appear affected in AD. Furthermore, lower CSF  $A\beta_{1-42}$  and higher p-tau<sub>181p</sub> concentrations were associated with an increase in the rate of ventricular expansion in controls; (2) in MCI subjects, an association was observed between increased CSF tau and decreased baseline caudate volume as well as between lower CSF  $A\beta_{1-42}$  and increased ventricular enlargement. In addition, lower CSF  $A\beta_{1-42}$  and higher p-tau<sub>181p</sub> and t-tau concentrations were associated with higher rates of brain volume loss in regions of the temporal

and parietal cortices and in subcortical regions implicated in AD pathology; (3) in AD patients, lower CSF  $A\beta_{1-42}$  concentration was associated with a decrease in volumes of brain regions not typically implicated in the amyloid pathology of AD. Specifically, lower CSF  $A\beta_{1-42}$  was associated with reduced atrophy rates in caudate and accumbens areas. On the other hand, higher t-tau concentration was associated with increased atrophy rates in regions of the posterior cingulate and precuneus, decreased atrophy rate in caudate, and decreased rate of ventricular enlargement; and (4) the relationship among CSF biomarkers, ApoE  $\epsilon 4$  status, and brain atrophy rates was regionally specific and varied across the clinical groups.

Our finding in controls, demonstrating that low baseline CSF  $A\beta_{1-42}$  biomarker concentration is associated with thinner cortex predominantly in the inferior temporal, parietal, frontal, precuneus, and posterior cingulate cortices, provides evidence for a link between variations in peripheral CSF chemistry and regional brain size. Moreover, the result suggests that the link between CSF markers and regional brain size is already established in absence of any apparent clinical symptoms of cognitive deficits. A previous study in cognitively normal elderly also found an association between low levels of CSF  $A\beta_{1-42}$  and smaller whole-brain volume (Fagan et al., 2009). It has been shown that in healthy elderly individuals, reduction in CSF  $A\beta_{1-42}$  is a predictor of cognitive decline and development of AD (Skogog et al., 2003; Stomrud et al., 2007); therefore, the association between low baseline CSF  $A\beta_{1-42}$  concentration and thin cortex in controls could reflect preclinical AD pathology. However, pathological conditions other than AD might also contribute to the relationship between low CSF  $A\beta_{1-42}$  concentration and cortical thinning.

Another interesting observation in controls is the association between variations in CSF  $A\beta_{1-42}$  and p-tau<sub>181p</sub> concentrations and the rate of ventricular dilation. There are several explanations for this finding. First, the associations may reflect early brain changes associated with AD pathology before clinical symptoms of dementia become apparent and ventricular dilation may reflect the combinations of all these brain changes, which are likely distributed diffusely throughout the brain at this early stage and therefore difficult to detect with conventional techniques of imaging statistics. Another explanation is that the association between CSF and structural changes in controls are not specifically related to AD pathology but merely reflect a general trend of a relationship between CSF biomarker concentrations and brain structures, including other pathologies that can lead to neurodegeneration such as cerebrovascular diseases. It will be important in future studies to determine the predictive value of the relationship between low CSF  $A\beta_{1-42}$  and high CSF p-tau<sub>181p</sub> and ventricular dilatation in controls for the development of AD pathology.

Individuals with MCI displayed associations between CSF p-tau<sub>181p</sub> and t-tau concentrations and baseline volume

of subcortical structures, specifically the caudate, while other baseline regional brain volumes or cortical thickness measures had no significant association with CSF biomarker concentrations. This finding implies a dissociation between CSF biomarkers and their effects on the brain in individuals with MCI. The finding in MCI, showing that variations in CSF biomarker concentrations are associated with a characteristic pattern of altered rates of regional brain atrophy, similar to the pattern seen in AD, further supports the view that these relations reflect brain alterations presymptomatic to AD and could be useful for staging disease severity and assessing disease progression. Specifically, lower CSF  $A\beta_{1-42}$  and increased CSF p-tau<sub>181p</sub> and t-tau concentrations in MCI were associated with higher atrophy rates both in terms of tissue volume loss and cortical thinning involving primarily inferior and medial temporal, parietal, precuneus, and posterior cingulate cortices and tissue volume loss in subcortical structures, including hippocampus, amygdala, and enlargement of ventricles. Structural MRI studies in AD consistently revealed a pattern of neuroanatomic abnormalities that predominantly involves structures in the medial temporal cortex (i.e., hippocampus and the entorhinal cortex [deToledo-Morrell et al., 2004; Du et al., 2001, 2003, 2004; Hampel et al., 2005; Morra et al., 2008, 2009a, 2009b; Schroeter et al., 2009; Stoub et al., 2005; Thompson et al., 2004]) where the early pathological changes are seen, then gradually extends to temporoparietal cortical areas (Chetelat and Baron, 2003; Desikan et al., 2008; Hua et al., 2008; Whitwell et al., 2007, 2008) as severity of AD progresses (deCarli et al., 2007; Jack et al., 2004, 2005, 2008b; Whitwell et al., 2007, 2008). Our finding that lower CSF  $A\beta_{1-42}$  and higher CSF p-tau<sub>181p</sub> and t-tau concentrations were associated with higher atrophy rates of the temporal horn and inferior temporal lobe regions points to a selective vulnerability of these regions to AD pathology, consistent with histopathological findings. The finding that lower CSF  $A\beta_{1-42}$  is associated with a characteristic pattern of brain atrophy in MCI that resembles the atrophy pattern seen in AD is encouraging for the use of CSF  $A\beta_{1-42}$  as an early indicator of AD. Most importantly, elucidating the detrimental relationship between CSF biomarkers and rates of brain atrophy is of great interest to detect AD pathology in early stage, which is fundamental for an accurate early diagnosis of the disease, development of new treatment interventions, and evaluation of clinical trials in AD. The synergistic relationship between CSF biomarker and neurodegeneration patterns are of clinical interest as they may not only improve monitoring AD progression and evaluation of new AD therapies but also aid enrichment of clinical trial cohorts by identifying specific subsets of patients with MCI especially at high risk of developing AD (Blennow and Hampel, 2003; Hampel et al., 2003; John, 2001). Such a custom-tailored cohort selection is desirable because drugs with disease-arresting effects have better efficacy in the

preclinical and early phase of the disease before the synaptic and neuronal loss become widespread (Shaw et al., 2007).

The spatial extent of baseline CSF  $A\beta_{1-42}$  modulation effects on brain atrophy and ventricular expansion observed in individuals with MCI is consistent with previous volumetric studies on patterns of increased atrophy rate in AD patients compared with elderly healthy controls (Scahill et al., 2002). In addition, a prior autopsy study on AD patients (Arnold et al., 1991) reported neuritic plaques distributed throughout the cortex with the highest densities in the temporal and occipital lobes, while relatively lower plaque densities were found in the parietal lobe. This is consistent with our CSF  $A\beta_{1-42}$  modulation effect findings in MCI. Compared with the prior autopsy study in AD patients (Arnold et al., 1991), the spatial extents of CSF p-tau<sub>181p</sub> and t-tau modulation effects are consistent with the neurofibrillary tangle distributions in AD pathology. In particular, hippocampus and cortical regions surrounding entorhinal cortex and amygdala were reported as the most severely affected areas by neurofibrillary tangles. However, because we do not know how many of the MCI subjects in this study will ultimately develop AD, we cannot determine the predictive value of CSF biomarker concentrations for AD. Another observation in the MCI group was the left hemisphere dominance of the CSF biomarkers' atrophy modulation effects. This observation is consistent with the asymmetric loss of gray matter (i.e., the left hemisphere atrophies faster than the right hemisphere) in AD (Thompson et al., 2003) and yet again supporting the hypothesis that CSF  $A\beta_{1-42}$ , p-tau<sub>181p</sub>, and t-tau are measures of early AD pathology.

In AD patients, lower baseline CSF  $A\beta_{1-42}$  concentration is associated with smaller baseline gray matter tissue volumes in lingual, pericalcarine, and postcentral cortices, which are not traditionally associated with AD pathology. Another surprising finding in AD patients was that abnormal CSF biomarker levels were not significantly associated with rates of cortical thinning, despite positive findings of an association between CSF  $A\beta_{1-42}$ , as well as t-tau levels and rates of volume loss in the caudate, posterior cingulate, and precuneus. Similarly, abnormal CSF biomarker levels in controls were also not significantly associated with rates of cortical thinning but showed an association with ventricular enlargement. The difference between the CSF biomarker relations to cortical thinning and volume loss could be related to differences in MRI sensitivity for detection of volume loss versus cortical thinning. It is also plausible, however, that the difference in AD is the result of a complex relationship between advanced AD pathology in most cortical regions and peripheral biomarker concentration, while the difference in controls might reflect a threshold effect of minimum biomarker concentration on cortical thinning and volume loss. More studies are warranted to further investigate these issues.

Compared with CN and MCI groups, CSF biomarker concentrations have opposite modulation effects on rates of

brain tissue volume change in AD. Specifically, we observed decreased rates of atrophy in the caudate and accumbens area in the presence of lower concentrations of CSF  $A\beta_{1-42}$  (relative to the CSF  $A\beta_{1-42}$  concentration distribution in the AD group), as well as decreased rates of atrophy in the right posterior cingulate and precuneus cortices and ventricular enlargement in the presence of higher concentrations of baseline CSF t-tau (relative to the CSF t-tau concentration distribution in the AD group). Although not statistically significant, similar trends were observed in cortical atrophy analysis as well, as shown in the supplementary figure. One explanation of this finding could be the disease-stage specific effects of CSF biomarkers on brain atrophy. AD subjects with lower CSF  $A\beta_{1-42}$  and higher CSF t-tau concentrations (relative to the biomarker concentration distributions in the AD group) probably have advanced AD pathology where they reach a plateau in their rates of volume loss, which appear as a slower progression of the brain atrophy.

An interesting finding was that relations between the rate of brain atrophy and CSF biomarker concentrations varied across the CSF  $A\beta_{1-42}$ , p-tau<sub>181p</sub>, and t-tau. This is not unexpected because it is known that amyloid plaques and tau-containing tangles are distributed discordantly in brain at early stages of the disease. Specifically, the accumulation of amyloid plaques occurs in cortical regions whereas tangles appear in subcortical structures, predominantly involving the hippocampus (Arnold et al., 1991; Braak and Braak, 1991; Price and Morris, 1999). Our findings reflect this pattern to some extent. However, the association between elevated CSF tau concentration and caudate atrophy in MCI and AD is an unexpected finding. Recent amyloid imaging studies using <sup>11</sup>C-labeled Pittsburgh Compound-B positron emission tomography (11C PiB-PET) reported substantial amyloid deposition in the striatum, including the caudate, in symptomatic and asymptomatic subjects carrying the presenilin-1 (PS1) mutation gene for familial AD (Klunk et al., 2007). It is therefore possible that our finding with respect to caudate atrophy can be explained by the heterogeneity of MCI and AD study groups, which might include subjects with early onset AD.

Finally, the finding of regional variations among CSF biomarkers, ApoE  $\epsilon$ 4 status, and brain atrophy rate relationships support the view that the genetic predisposition of the brain to amyloid and tau mediated pathology is region and disease stage specific. Interestingly, the most prominent region associated with CSF biomarker regardless of ApoE  $\epsilon$ 4 status in MCI included the entorhinal cortex, which is thought to be affected early by AD. Moreover, the effect of ApoE  $\epsilon$ 4 status on the relationships could be dose-dependent (Andersson et al., 2007; Glodzik-Sobanska et al., 2009; Sunderland et al., 2004).

Our findings in this study are largely consistent with several similar studies on relationships between CSF biomarkers and brain alterations in MCI and AD (Hampel et

al., 2005; Henneman et al., 2009; Herukka et al., 2008). Specifically, increased concentrations of CSF p-tau<sub>181p</sub> are associated with higher subsequent rates of hippocampal atrophy in the progressive MCI and AD patients (Hampel et al., 2005; Henneman et al., 2009; Herukka et al., 2008), of medial temporal atrophy in AD patients (Leow et al., 2009), of the temporal and parietal atrophy in MCI (Fjell et al., 2010b), and of right posterior ventricular horn expansion (Chou et al., 2009). In contrast, low CSF  $A\beta_{1-42}$  concentration exhibited an association with increased rate of left hippocampal atrophy in the progressive MCI patients (Fjell et al., 2010b; Herukka et al., 2008), of the medial temporal atrophy in AD (Leow et al., 2009), of the temporal and parietal atrophy in MCI (Fjell et al., 2010b), and of ventricular expansion (Chou et al., 2009). Elevated CSF t-tau concentrations are associated with higher rates of hippocampal atrophy in stable MCI patients (Herukka et al., 2008). In controls, it has been shown that low CSF  $A\beta_{1-42}$  concentration correlates with ventricular expansion and volumetric reductions in widespread brain areas, including inferior temporal, inferior parietal, frontal, posterior cingulate, precuneus, caudate, and amygdala regions (Fjell et al., 2010a). Fjell et al. reported generally larger effects of CSF biomarkers on brain tissue change than what we found on the same cohort (Fjell et al., 2010a, 2010b). However, several methodological differences between our study and that by Fjell et al. complicate direct comparisons. For example, whereas Fjell et al. aimed to evaluate potentially accelerated rates between the first and second scan intervals while accepting mixed effects on rates, we aimed to separate random from fixed effects on rates to boost sensitivity while ignoring the possibility of accelerated rates. Because each approach has its estimation bias, the different findings are difficult to interpret.

The majority of previous MRI studies, except Fjell et al. (2010a, 2010b), in this context focused on the hippocampal and temporal lobe atrophy and ventricular enlargement, while our approach was generalized by assessing various other brain regions. Based on this, we discovered that the association between CSF biomarkers and structural changes are regionally differential. Although this observation is not entirely surprising, given that the pathological processes of plaque and tangle formation, which CSF  $A\beta_{1-42}$  and p-tau<sub>181p</sub> and t-tau indirectly represent, respectively. The finding of faster progression of brain atrophy in presence of lower baseline concentrations of  $A\beta_{1-42}$  and higher concentrations of p-tau<sub>181p</sub>/t-tau in MCI together with the similarities between the MCI pattern of CSF biomarker atrophy modulation effects and distribution of tangles and plaques in AD support the hypothesis that CSF biomarkers are measures of early AD pathology. MCI pattern of relations between rate of brain atrophy and CSF biomarker concentrations should be further explored to identify possible presymptomatic AD pathology. This finding also suggests a strategy for the potential use of biomarkers in clinical trials.

For example, CSF  $A\beta_{1-42}$  concentration could be used to assess the effect of disease-modifying interventions on cortical regions while CSF p-tau<sub>181p</sub> and t-tau concentrations could be used to assess effects on subcortical structures, while both biomarkers could be used together to determine if interventions affect cortical and subcortical brain structures differentially. CSF biomarker cutoffs to select fastest progressing cohorts could greatly improve the power of AD prevention trials on healthy elderly and MCI.

Several limitations of our study ought to be mentioned. First, MCI and AD subjects were diagnosed clinically; therefore other pathologies may have contributed to their symptoms and the relationships between CSF biomarkers and brain alterations may be unrelated to AD pathology. Another limitation is that CSF biomarkers, especially CSF  $A\beta_{1-42}$ , have been shown to be saturated and may not accurately reflect severity of brain amyloid deposition or plaque density in the later stages of the disease (Andreasen et al., 1999; Stefani et al., 2006). Therefore, structural brain changes may still occur secondarily to ongoing amyloid deposition or plaque accumulation. Restriction to linear, time-invariant brain atrophy rates is a technical limitation of our study. This is likely a gross simplification because the loss of brain tissue may be compounding and furthermore neurodegeneration in AD may be a dynamic process, which varies during disease progression. Therefore, models with nonlinear atrophy rate characteristics might lead to different results; however, such models are not always robust, given the limited number of serial MRI measurements and they also require careful validation. Finally, another technical limitation is that our study included fewer CN than MCI subjects despite expectations that power to detect atrophy will be higher for MCI than in CN because of higher atrophy rates in MCI. Therefore, comparisons between CN and MCI (and AD) could be biased toward lower sensitivity to detect a change in CN.

In summary, our findings demonstrate that alterations in CSF  $A\beta_{1-42}$ , p-tau<sub>181p</sub>, and t-tau are each associated with characteristic patterns of structural brain changes (cross-sectionally or longitudinally) in CN and MCI that resembles to a large extent the pattern seen in AD pathology. Specifically, the finding of faster progression of brain atrophy in individuals with MCI in the presence of lower baseline CSF  $A\beta_{1-42}$  and higher CSF tau levels supports the view that these CSF biomarkers reflect AD brain pathology. Because the CSF  $A\beta_{1-42}$  and tau levels were also associated with a systematic pattern of regional brain atrophy rates that resembled the pattern known in AD, our findings further support the view that CSF  $A\beta_{1-42}$  and tau reflect brain damage due to AD pathology. Overall, the findings imply that CSF  $A\beta_{1-42}$  and tau taken together with MRI measures of rates of brain atrophy progression are promising candidates as biomarkers for early detection of AD.

## Disclosure statement

Dr. Tosun, Ms. Truran-Sacrey, Dr. Shaw, and Dr. Trojanowski report no disclosures.

Dr. Schuff received honoraria from the Michael J. Fox foundation, the British Research Council, and Elsevier Publishing company; receives research support from The Michael J. Fox foundation, and Department of Defense (WX), P41 RR023953 (Coinvestigator); P50AG23501 (Coinvestigator).

Dr. Aisen has served as a consultant to Pfizer, Merck, and Novartis.

Dr. Petersen serves as a consultant to Elan Pharmaceuticals, Wyeth Pharmaceuticals, and GE Healthcare; receives royalties from publishing *Mild Cognitive Impairment* (Oxford University Press, 2003); and receives research support from the NIA [AG 06786 (PI) and AG 16,574 (PI)].

Dr. Weiner serves on scientific advisory boards for Bayer Schering Pharma, Eli Lilly, Nestle, CoMentis, Neurochem, Eisai, Avid, Aegis, Genentech, Allergan, Lippincott, Bristol Meyers Squibb, Forest, Pfizer, McKinsey, Mitsubishi, and Novartis. He has received nonindustry-supported funding for travel; serves on the editorial board of *Alzheimer's & Dementia*; received honoraria from the Rotman Research Institute and BOLT International; receives research support from Merck & Co, Avid, NIH [U01AG024904 (PI), P41 RR023953 (PI), R01 AG10897 (PI), P01AG19724 (Coinvestigator), P50AG23501 (Coinvestigator), R24 RR021992 (Coinvestigator), R01 NS031966 (Coinvestigator), and P01AG012435 (Coinvestigator)], the Department of Defense [DAMD17-01-1-0764 (PI)], and the Veterans Administration [MIRECC VISN 21 (Core PI)]; and holds stock in Synarc and Elan Pharmaceuticals.

Written consent was obtained from all subjects participating in the study according to the Declaration of Helsinki, and the study was approved by the institutional review board at each participating site.

## Acknowledgements

Data used in the preparation of this article were obtained from the Alzheimer's Disease Neuroimaging Initiative (ADNI) database ([www.loni.ucla.edu/ADNI](http://www.loni.ucla.edu/ADNI)). As such, the investigators within the ADNI contributed to the design and implementation of ADNI and/or provided data but did not participate in analysis or writing of this report. Complete listing of ADNI investigators is available at [http://www.loni.ucla.edu/ADNI/Collaboration/ADNI\\_Manuscript\\_Citations.pdf](http://www.loni.ucla.edu/ADNI/Collaboration/ADNI_Manuscript_Citations.pdf).

This work is funded by the National Institutes of Health (NIH), National Institute of Biomedical Imaging and Bioengineering (NIBIB) [T32 EB001631-05].

Data collection and sharing for this project was funded by the Alzheimer's disease Neuroimaging Initiative (ADNI) (National Institutes of Health, Grant U01 AG024904).

ADNI is funded by the National Institute on Aging, the National Institute of Biomedical Imaging and Bioengineering, and through generous contributions from the following: Abbott, AstraZeneca AB, Bayer Schering Pharma AG, Bristol-Myers Squibb, Eisai Global Clinical Development, Elan Corporation, Genentech, GE Healthcare, GlaxoSmithKline, Innogenetics, Johnson and Johnson, Eli Lilly, and Co., Medpace, Inc., Merck and Co., Inc., Novartis AG, Pfizer Inc, F. Hoffman-La Roche, Schering-Plough, Synarc, Inc., and Wyeth, as well as nonprofit partners the Alzheimer's Association and Alzheimer's Drug Discovery Foundation, with participation from the US Food and Drug Administration. Private sector contributions to ADNI are facilitated by the Foundation for the National Institutes of Health ([www.fnih.org/](http://www.fnih.org/)). The grantee organization is the Northern California Institute for Research and Education, and the study is coordinated by the Alzheimer's Disease Cooperative Study at the University of California, San Diego. ADNI data are disseminated by the Laboratory for Neuro Imaging at the University of California, Los Angeles. This research was also supported by NIH grants P30 AG010129, K01 AG030514, and the Dana Foundation.

#### Appendix. Supplementary data

Supplementary data associated with this article can be found, in the online version, at [doi:10.1016/j.neurobiolaging.2010.04.030](https://doi.org/10.1016/j.neurobiolaging.2010.04.030).

#### References

- Aizenstein, H.J., Nebes, R.D., Saxton, J.A., Price, J.C., Mathis, C.A., Tsopelas, N.D., Ziolkowski, S.K., James, J.A., Snitz, B.E., Houck, P.R., Bi, W., Cohen, A.D., Lopresti, B.J., deKosky, S.T., Halligan, E.M., Klunk, W.E., 2008. Frequent amyloid deposition without significant cognitive impairment among the elderly. *Arch. Neurol.* 65, 1509–1517.
- Andersson, C., Blennow, K., Johansson, S.E., Almkvist, O., Engfeldt, P., Lindau, M., Eriksdotter-Jonhagen, M., 2007. Differential CSF biomarker levels in APOE-ε4-positive and -negative patients with memory impairment. *Dement. Geriatr. Cognit. Disord.* 23, 87–95.
- Andreasen, N., Minthon, L., Vanmechelen, E., Vanderstichele, H., Davidsson, P., Winblad, B., Blennow, K., 1999. Cerebrospinal fluid tau and A[β]42 as predictors of development of Alzheimer's disease in patients with mild cognitive impairment. *Neurosci. Lett.* 273, 5–8.
- Arnold, S.E., Hyman, B.T., Flory, J., Damasio, A.R., Van Hoesen, G.W., 1991. The topographical and neuroanatomical distribution of neurofibrillary tangles and neuritic plaques in the cerebral cortex of patients with Alzheimer's disease. *Cereb. Cortex* 1, 103–116.
- Basso, M., Gelernter, J., Yang, J., MacAvoy, M.G., Varma, P., Bronen, R.A., van Dyck, C.H., 2006. Apolipoprotein E ε4 is associated with atrophy of the amygdala in Alzheimer's disease. *Neurobiol. Aging* 27, 1416–1424.
- Benjamini, Y., Hochberg, Y., 1995. Controlling the false discovery rate: a practical and powerful approach to multiple testing. *J. R. Stat. Soc. B Stat. Methodol.* 57, 289–300.
- Blennow, K., Hampel, H., 2003. CSF markers for incipient Alzheimer's disease. *Lancet Neurol.* 2, 605–613.
- Braak, H., Braak, E., 1991. Neuropathological staging of Alzheimer-related changes. *Acta Neuropathol.* 82, 239–259.
- Brys, M., Glodzik, L., Mosconi, L., Switalski, R., De Santi, S., Pirraglia, E., Rich, K., Kim, B.C., Mehta, P., Zinkowski, R., Pratico, D., Wallin, A., Zetterberg, H., Tsui, W.H., Rusinek, H., Blennow, K., de Leon, M.J., 2009. Magnetic resonance imaging improves cerebrospinal fluid biomarkers in the early detection of Alzheimer's disease. *J. Alzheimers Dis.* 16, 351–362.
- Chetelat, G.A., Baron, J.-C., 2003. Early diagnosis of Alzheimer's disease: contribution of structural neuroimaging. *Neuroimage* 18, 525–541.
- Chou, Y.-Y., Lopor, È.N., Avedissian, C., Madsen, S.K., Parikshak, N., Hua, X., Shaw, L.M., Trojanowski, J.Q., Weiner, M.W., Toga, A.W., Thompson, P.M., 2009. Mapping correlations between ventricular expansion and CSF amyloid and tau biomarkers in 240 subjects with Alzheimer's disease, mild cognitive impairment and elderly controls. *Neuroimage* 46, 394–410.
- Clark, C.M., Xie, S., Chittams, J., Ewbank, D., Peskind, E., Galasko, D., Morris, J.C., McKeel, D.W., Jr, Farlow, M., Weitlauf, S.L., Quinn, J., Kaye, J., Knopman, D., Arai, H., Doody, R.S., deCarli, C., Leight, S., Lee, V.M.-Y., Trojanowski, J.Q., 2003. Cerebrospinal fluid tau and beta-amyloid: how well do these biomarkers reflect autopsy-confirmed dementia diagnoses? *Arch. Neurol.* 60, 1696–1702.
- deCarli, C., Frisoni, G.B., Clark, C.M., Harvey, D., Grundman, M., Petersen, R.C., Thal, L.J., Jin, S., Jack, C.R., Jr, Scheltens, P., for the Alzheimer's Disease Cooperative Study Group, 2007. Qualitative estimates of medial temporal atrophy as a predictor of progression from mild cognitive impairment to dementia. *Arch. Neurol.* 64, 108–115.
- Desikan, R.S., Fischl, B., Cabral, H.J., Kemper, T.L., Guttman, C.R.G., Blacker, D., Hyman, B.T., Albert, M.S., Killiany, R.J., 2008. MRI measures of temporoparietal regions show differential rates of atrophy during prodromal AD. *Neurology* 71, 819–825.
- deToledo-Morrell, L., Stoub, T.R., Bulgakova, M., Wilson, R.S., Bennett, D.A., Leurgans, S., Wu, J., Turner, D.A., 2004. MRI-derived entorhinal volume is a good predictor of conversion from MCI to AD. *Neurobiol. Aging* 25, 1197–1203.
- Du, A.T., Schuff, N., Amend, D., Laakso, M.P., Hsu, Y.Y., Jagust, W.J., Yaffe, K., Kramer, J.H., Reed, B., Norman, D., Chui, H.C., Weiner, M.W., 2001. Magnetic resonance imaging of the entorhinal cortex and hippocampus in mild cognitive impairment and Alzheimer's disease. *J. Neurol. Neurosurg. Psychiatry* 71, 441–447.
- Du, A.T., Schuff, N., Kramer, J.H., Ganzer, S., Zhu, X.P., Jagust, W.J., Miller, B.L., Reed, B.R., Mungas, D., Yaffe, K., Chui, H.C., Weiner, M.W., 2004. Higher atrophy rate of entorhinal cortex than hippocampus in AD. *Neurology* 62, 422–427.
- Du, A.T., Schuff, N., Laakso, M.P., Zhu, X.P., Jagust, W.J., Yaffe, K., Kramer, J.H., Miller, B.L., Reed, B.R., Norman, D., Chui, H.C., Weiner, M.W., 2002. Effects of subcortical ischemic vascular dementia and AD on entorhinal cortex and hippocampus. *Neurology* 58, 1635–1641.
- Du, A.T., Schuff, N., Zhu, X.P., Jagust, W.J., Miller, B.L., Reed, B.R., Kramer, J.H., Mungas, D., Yaffe, K., Chui, H.C., Weiner, M.W., 2003. Atrophy rates of entorhinal cortex in AD and normal aging. *Neurology* 60, 481–486.
- Duarte, A., Hayasaka, S., Du, A., Schuff, N., Jahng, G.-H., Kramer, J., Miller, B., Weiner, M., 2006. Volumetric correlates of memory and executive function in normal elderly, mild cognitive impairment and Alzheimer's disease. *Neurosci. Lett.* 406, 60–65.
- Fagan, A.M., Head, D., Shah, A.R., Marcus, D., Mintun, M., Morris, J.C., Holtzman, D.M., 2009. Decreased cerebrospinal fluid Aβ(42) correlates with brain atrophy in cognitively normal elderly. *Ann. Neurol.* 65, 176–183.
- Fischl, B., Dale, A.M., 2000. Measuring the thickness of the human cerebral cortex from magnetic resonance images. *Proc. Natl. Acad. Sci. U. S. A.* 97, 11050–11055.
- Fischl, B., Salat, D.H., Busa, E., Albert, M., Dieterich, M., Haselgrove, C., van der Kouwe, A., Killiany, R., Kennedy, D., Klaveness, S., Montillo, A., Makris, N., Rosen, B., Dale, A.M., 2002. Whole brain segmentation: automated labeling of neuroanatomical structures in the human brain. *Neuron* 33, 341–355.
- Fischl, B., van der Kouwe, A., Destrieux, C., Halgren, E., Segonne, F., Salat, D.H., Busa, E., Seidman, L.J., Goldstein, J., Kennedy, D., Cavi-

- ness, V., Makris, N., Rosen, B., Dale, A.M., 2004. Automatically parcellating the human cerebral cortex. *Cereb. Cortex* 14, 11–22.
- Fjell, A.M., Walhovd, K.B., Amlien, I., Bjornerud, A., Reinvang, I., Gjerstad, L., Cappelen, T., Willoch, F., Due-Tønnessen, P., Grambaite, R., Skinningsrud, A., Stenset, V., Fladby, T., 2008. Morphometric changes in the episodic memory network and tau pathologic features correlate with memory performance in patients with mild cognitive impairment. *AJNR Am. J. Neuroradiol.* 29, 1183–1189.
- Fjell, A.M., Walhovd, K.B., Fennema-Notestine, C., McEvoy, L.K., Hagler, D.J., Holland, D., Blennow, K., Brewer, J.B., Dale, A.M., Alzheimer's Disease Neuroimaging Initiative, 2010a. Brain atrophy in healthy aging is related to CSF levels of A $\beta$ <sub>1–42</sub>. *Cereb. Cortex*, in press doi:10.1093/cercor/bhp279.
- Fjell, A.M., Walhovd, K.B., Fennema-Notestine, C., McEvoy, L.K., Hagler, D.J., Holland, D., Brewer, J.B., Dale, A.M., Alzheimer's Disease Neuroimaging Initiative, 2010b. CSF biomarkers in prediction of cerebral and clinical change in mild cognitive impairment and Alzheimer's disease. *J. Neurosci.* 30, 2088–2101.
- Fleisher, A., Grundman, M., Jack, C.R., Jr, Petersen, R.C., Taylor, C., Kim, H.T., Schiller, D.H.B., Bagwell, V., Sencakova, D., Weiner, M.F., deCarli, C., deKosky, S.T., van Dyck, C.H., Thal, L.J., for the Alzheimer's Disease Cooperative Study, 2005. Sex, apolipoprotein E {varepsilon}4 status, and hippocampal volume in mild cognitive impairment. *Arch Neurol* 62, 953–957.
- Glodzik-Sobanska, L., Pirraglia, E., Brys, M., de Santi, S., Mosconi, L., Rich, K.E., Switalski, R., Louis, L.S., Sadowski, M.J., Martiniuk, F., Mehta, P., Pratico, D., Zinkowski, R.P., Blennow, K., de Leon, M.J., 2009. The effects of normal aging and ApoE genotype on the levels of CSF biomarkers for Alzheimer's disease. *Neurobiol. Aging* 30, 672–681.
- Hampel, H., Burger, K., Pruessner, J.C., Zinkowski, R., deBernardis, J., Kerkman, D., Leinsinger, G., Evans, A.C., Davies, P., Moller, H.-J., Teipel, S.J., 2005. Correlation of cerebrospinal fluid levels of tau protein phosphorylated at threonine 231 with rates of hippocampal atrophy in Alzheimer disease. *Arch. Neurol.* 62, 770–773.
- Hampel, H., Teipel, S.J., Fuchsberger, T., Andreasen, N., Wiltfang, J., Otto, M., Shen, Y., Dodel, R., Du, Y., Farlow, M., Moller, H.J., Blennow, K., Buerger, K., 2003. Value of CSF  $\tau$  amyloid<sub>1–42</sub> and tau as predictors of Alzheimer's disease in patients with mild cognitive impairment. *Mol. Psychiatry* 9, 705–710.
- Henneman, W.J.P., Vrenken, H., Barnes, J., Sluimer, I.C., Verwey, N.A., Blankenstein, M.A., Klein, M., Fox, N.C., Scheltens, P., Barkhof, F., van der Flier, W.M., 2009. Baseline CSF p-tau levels independently predict progression of hippocampal atrophy in Alzheimer disease. *Neurology* 73, 935–940.
- Herukka, S.-K., Pennanen, C., Soininen, H., Pirttilä, T., 2008. CSF A $\beta$ <sub>42</sub>, Tau and Phosphorylated Tau Correlate with Medial Temporal Lobe Atrophy. *J. Alzheimers Dis.* 14, 51–57.
- Hua, X., Leow, A.D., Lee, S., Klunder, A.D., Toga, A.W., Lepore, N., Chou, Y.-Y., Brun, C., Chiang, M.-C., Barysheva, M., Jack, C.R., Jr, Bernstein, M.A., Britson, P.J., Ward, C.P., Whitwell, J.L., Borowski, B., Fleisher, A.S., Fox, N.C., Boyes, R.G., Barnes, J., Harvey, D., Kornak, J., Schuff, N., Boreta, L., Alexander, G.E., Weiner, M.W., Thompson, P.M., Alzheimer's Disease Neuroimaging Initiative, 2008. 3D characterization of brain atrophy in Alzheimer's disease and mild cognitive impairment using tensor-based morphometry. *Neuroimage* 41, 19–34.
- Jack, C.R., Bernstein, M.A., Fox, N.C., Thompson, P., Alexander, G., Harvey, D., Borowski, B., Britson, P.J., Whitwell, J.L., Ward, C., Dale, A.M., Felmlee, J.P., Gunter, J.L., Hill, D.L.G., Killiany, R., Schuff, N., Fox-Bosetti, S., Lin, C., Studholme, C., deCarli, C.S., Krueger, G., Ward, H.A., Metzger, G.J., Scott, K.T., Mallozzi, R., Blezek, D., Levy, J., Debbs, J.P., Fleisher, A.S., Albert, M., Green, R., Bartzokis, G., Glover, G., Mugler, J., Weiner, M.W., 2008a. The Alzheimer's Disease Neuroimaging Initiative (ADNI): MRI methods. *J. Mag. Reson. Imaging* 27, 685–691.
- Jack, C.R., Jr, Lowe, V.J., Weigand, S.D., Wiste, H.J., Senjem, M.L., Knopman, D.S., Shiung, M.M., Gunter, J.L., Boeve, B.F., Kemp, B.J., Weiner, M., Petersen, R.C., Alzheimer's Disease Neuroimaging Initiative, 2009. Serial PIB and MRI in normal, mild cognitive impairment and Alzheimer's disease: implications for sequence of pathological events in Alzheimer's disease. *Brain* 132, 1355–1365.
- Jack, C.R., Jr, Shiung, M.M., Weigand, S.D., O'Brien, P.C., Gunter, J.L., Boeve, B.F., Knopman, D.S., Smith, G.E., Ivnik, R.J., Tangalos, E.G., Petersen, R.C., 2005. Brain atrophy rates predict subsequent clinical conversion in normal elderly and amnesic MCI. *Neurology* 65, 1227–1231.
- Jack, C.R., Jr, Weigand, S.D., Shiung, M.M., Przybelski, S.A., O'Brien, P.C., Gunter, J.L., Knopman, D.S., Boeve, B.F., Smith, G.E., Petersen, R.C., 2008b. Atrophy rates accelerate in amnesic mild cognitive impairment. *Neurology* 70, 1740–1752.
- Jack, C.R., Jr, Shiung, M.M., Gunter, J.L., O'Brien, P.C., Weigand, S.D., Knopman, D.S., Boeve, B.F., Ivnik, R.J., Smith, G.E., Cha, R.H., Tangalos, E.G., Petersen, R.C., 2004. Comparison of different MRI brain atrophy rate measures with clinical disease progression in AD. *Neurology* 62, 591–600.
- John, H.G., 2001. Incorporating biomarkers into clinical drug trials in Alzheimer's disease. *J. Alzheimers Dis.* 3, 287–292.
- Klunk, W.E., Price, J.C., Mathis, C.A., Tsopelas, N.D., Lopresti, B.J., Ziolko, S.K., Bi, W., Hoge, J.A., Cohen, A.D., Ikonovic, M.D., Saxton, J.A., Snitz, B.E., Pollen, D.A., Moonis, M., Lippa, C.F., Swearer, J.M., Johnson, K.A., Rentz, D.M., Fischman, A.J., Aizenstein, H.J., deKosky, S.T., 2007. Amyloid deposition begins in the striatum of presenilin-1 mutation carriers from two unrelated pedigrees. *J. Neurosci.* 27, 6174–6184.
- Kramer, J.H., Schuff, N., Reed, B.R., Mungas, D., Du, A.-T., Rosen, H.J., Jagust, W.J., Miller, B.L., Weiner, M.W., Chui, H.C., 2004. Hippocampal volume and retention in Alzheimer's disease. *J. Int. Neuropsychol. Soc.* 10, 639–643.
- Leow, A.D., Yanovsky, I., Parikshak, N., Hua, X., Lee, S., Toga, A.W., Jack, C.R., Jr, Bernstein, M.A., Britson, P.J., Gunter, J.L., Ward, C.P., Borowski, B., Shaw, L.M., Trojanowski, J.Q., Fleisher, A.S., Harvey, D., Kornak, J., Schuff, N., Alexander, G.E., Weiner, M.W., Thompson, P.M., 2009. Alzheimer's Disease Neuroimaging Initiative: A one-year follow up study using tensor-based morphometry correlating degenerative rates, biomarkers and cognition. *Neuroimage* 45, 645–655.
- Mintun, M.A., laRossa, G.N., Sheline, Y.I., Dence, C.S., Lee, S.Y., Mach, R.H., Klunk, W.E., Mathis, C.A., deKosky, S.T., Morris, J.C., 2006. [<sup>11</sup>C]PIB in a nondemented population: potential antecedent marker of Alzheimer disease. *Neurology* 67, 446–452.
- Morra, J.H., Tu, Z., Apostolova, L.G., Green, A.E., Avedissian, C., Madsen, S.K., Parikshak, N., Hua, X., Toga, A.W., Jack, C.R., Jr, Weiner, M.W., Thompson, P.M., 2008. Validation of a fully automated 3D hippocampal segmentation method using subjects with Alzheimer's disease mild cognitive impairment, and elderly controls. *Neuroimage* 43, 59–68.
- Morra, J.H., Tu, Z., Apostolova, L.G., Green, A.E., Avedissian, C., Madsen, S.K., Parikshak, N., Hua, X., Toga, A.W., Jack, C.R., Jr, Schuff, N., Weiner, M.W., Thompson, P.M., Alzheimer's Disease Neuroimaging Initiative, 2009a. Automated 3D mapping of hippocampal atrophy and its clinical correlates in 400 subjects with Alzheimer's disease, mild cognitive impairment, and elderly controls. *Hum. Brain Mapp.* 30, 2766–2788.
- Morra, J.H., Tu, Z., Apostolova, L.G., Green, A.E., Avedissian, C., Madsen, S.K., Parikshak, N., Toga, A.W., Jack, C.R., Jr, Schuff, N., Weiner, M.W., Thompson, P.M., 2009b. Automated mapping of hippocampal atrophy in 1-year repeat MRI data from 490 subjects with Alzheimer's disease, mild cognitive impairment, and elderly controls. *Neuroimage* 45, S3–S15.
- Olsson, A., Vanderstichele, H., Andreasen, N., De Meyer, G., Wallin, A., Holmberg, B., Rosengren, L., Vanmechelen, E., Blennow, K., 2005. Simultaneous Measurement of  $\beta$  amyloid(1–42), total tau, and

- phosphorylated tau (Thr181) in cerebrospinal fluid by the xMAP Technology. *Clin. Chem.* 51, 336–345.
- Petersen, R.C., Smith, G.E., Waring, S.C., Ivnik, R.J., Tangalos, E.G., Kokmen, E., 1999. Mild cognitive impairment: clinical characterization and outcome. *Arch. Neurol.* 56, 303–308.
- Potkin, S.G., Guffanti, G., Lakatos, A., Turner, J.A., Kruggel, F., Fallon, J.H., Saykin, A.J., Orro, A., Lupoli, S., Salvi, E., Weiner, M., Macciardi, F., Alzheimer's Disease Neuroimaging Initiative, 2009. Hippocampal atrophy as a quantitative trait in a genome-wide association study identifying novel susceptibility genes for Alzheimer's disease. *PLoS One* 4, e6501.
- Price, J.L., Morris, J.C., 1999. Tangles and plaques in nondemented aging and "preclinical" Alzheimer's disease. *Ann. Neurol.* 45, 358–368.
- Scahill, R.L., Schott, J.M., Stevens, J.M., Rossor, M.N., Fox, N.C., 2002. Mapping the evolution of regional atrophy in Alzheimer's disease: Unbiased analysis of fluid-registered serial MRI. *Proc. Natl. Acad. Sci. U. S. A.* 99, 4703–4707.
- Schroeter, M.L., Stein, T., Maslowski, N., Neumann, J., 2009. Neural correlates of Alzheimer's disease and mild cognitive impairment: a systematic and quantitative meta-analysis involving 1351 patients. *Neuroimage* 47, 1196–1206.
- Schuff, N., Woerner, N., Boreta, L., Kornfield, T., Shaw, L.M., Trojanowski, J.Q., Thompson, P.M., Jack, C.R., Jr., Weiner, M.W., Alzheimer's Disease Neuroimaging Initiative, 2009. MRI of hippocampal volume loss in early Alzheimer's disease in relation to ApoE genotype and biomarkers. *Brain* 132, 1067–1077.
- Shaw, L.M., Korecka, M., Clark, C.M., Lee, V.M.Y., Trojanowski, J.Q., 2007. Biomarkers of neurodegeneration for diagnosis and monitoring therapeutics. *Nat. Rev. Drug Discov.* 6, 295–303.
- Shaw, L.M., Vanderstichele, H., Knapik-Czajka, M., Clark, C.M., Aisen, P.S., Petersen, R.C., Blennow, K., Soares, H., Simon, A., Lewczuk, P., Dean, R., Siemers, E., Potter, W., Lee, V.M.-Y., Trojanowski, J.Q., Initiative, A.S.D.N., 2009. Cerebrospinal fluid biomarker signature in Alzheimer's disease neuroimaging initiative subjects. *Ann. Neurol.* 65, 403–413.
- Skoog, I., Davidsson, P., Aevansson, O., Vanderstichele, H., Vanmechelen, E., Blennow, K., 2003. Cerebrospinal fluid beta-amyloid 42 is reduced before the onset of sporadic dementia: a population-based study in 85-year-olds. *Dement. Geriatr. Cogn. Disord.* 15, 169–176.
- Sluimer, J.D., Vrenken, H., Blankenstein, M.A., Fox, N.C., Scheltens, P., Barkhof, F., van der Flier, W.M., 2008. Whole-brain atrophy rate in Alzheimer disease: Identifying fast progressors. *Neurology* 70, 1836–1841.
- Stefani, A., Martorana, A., Bernardini, S., Panella, M., Mercati, F., Orlandino, A., Pierantozzi, M., 2006. CSF markers in Alzheimer disease patients are not related to the different degree of cognitive impairment. *J. Neurol. Sci.* 251, 124–128.
- Stomrud, E., Hansson, O., Blennow, K., Minthon, L., Londos, E., 2007. Cerebrospinal fluid biomarkers predict decline in subjective cognitive function over 3 years in healthy elderly. *Dement. Geriatr. Cogn. Disord.* 24, 118–124.
- Stoub, T.R., Bulgakova, M., Leurgans, S., Bennett, D.A., Fleischman, D., Turner, D.A., deToledo-Morrell, L., 2005. MRI predictors of risk of incident Alzheimer disease: a longitudinal study. *Neurology* 64, 1520–1524.
- Sunderland, T., Mirza, N., Putnam, K.T., Linker, G., Bhupali, D., Durham, R., Soares, H., Kimmel, L., Friedman, D., Bergeson, J., Csako, G., Levy, J.A., Bartko, J.J., Cohen, R.M., 2004. Cerebrospinal fluid-amyloid1-42 and tau in control subjects at risk for Alzheimer's disease: The effect of APOE 4 allele. *Biol. Psychiatry* 56, 670–676.
- Thompson, P.M., Hayashi, K.M., de Zubicaray, G., Janke, A.L., Rose, S.E., Semple, J., Herman, D., Hong, M.S., Dittmer, S.S., Doddrell, D.M., Toga, A.W., 2003. Dynamics of gray matter loss in Alzheimer's disease. *J. Neurosci.* 23, 994–1005.
- Thompson, P.M., Hayashi, K.M., de Zubicaray, G.I., Janke, A.L., Rose, S.E., Semple, J., Hong, M.S., Herman, D.H., Gravano, D., Doddrell, D.M., Toga, A.W., 2004. Mapping hippocampal and ventricular change in Alzheimer disease. *Neuroimage* 22, 1754–1766.
- Vemuri, P., Wiste, H.J., Weigand, S.D., Shaw, L.M., Trojanowski, J.Q., Weiner, M.W., Knopman, D.S., Petersen, R.C., Jack, C.R., Jr., Alzheimer's Disease Neuroimaging Initiative, 2009a. MRI and CSF biomarkers in normal, MCI, and AD subjects: diagnostic discrimination and cognitive correlations. *Neurology* 73, 287–293.
- Vemuri, P., Wiste, J., Weigand, S.D., Shaw, L.M., Trojanowski, J.Q., Weiner, M.W., Knopman, D.S., Petersen, R.C., Jack, C.R., Jr., Alzheimer's Disease Neuroimaging Initiative, 2009b. MRI and CSF biomarkers in normal, MCI, and AD subjects: predicting future clinical change. *Neurology* 73, 294–301.
- Whitwell, J.L., Przybelski, S.A., Weigand, S.D., Knopman, D.S., Boeve, B.F., Petersen, R.C., Jack, C.R., Jr., 2007. 3D maps from multiple MRI illustrate changing atrophy patterns as subjects progress from mild cognitive impairment to Alzheimer's disease. *Brain* 130, 1777–1786.
- Whitwell, J.L., Shiung, M.M., Przybelski, S.A., Weigand, S.D., Knopman, D.S., Boeve, B.F., Petersen, R.C., Jack, C.R., Jr., 2008. MRI patterns of atrophy associated with progression to AD in amnesic mild cognitive impairment. *Neurology* 70, 512–520.